

Genomic and metabolomic analysis of *Bacillus licheniformis* with enhanced poly- γ -glutamic acid production through atmospheric and room temperature plasma mutagenesis

Xiaoyu Wei¹, Lijie Yang¹, Haiyan Wang¹, Zhen Chen³, Yiyuan Xu¹, Yue Weng¹,
Mingfeng Cao¹, Qingbiao Li (✉)², Ning He (✉)¹

¹ Department of Chemical and Biochemical Engineering, College of Chemistry and Chemical Engineering,
Xiamen University, Xiamen 361005, China

² College of Food and Biological Engineering, Jimei University, Xiamen 361021, China

³ College of Life Science, Xinyang Normal University, Xinyang 464000, China

© Higher Education Press 2022

Abstract Poly- γ -glutamic acid is an extracellular polymeric substance with various applications owing to its valuable properties of biodegradability, flocculating activity, water solubility, and nontoxicity. However, the ability of natural strains to produce poly- γ -glutamic acid is low. Atmospheric and room temperature plasma was applied in this study to conduct mutation breeding of *Bacillus licheniformis* CGMCC 2876, and a mutant strain M32 with an 11% increase in poly- γ -glutamic acid was obtained. Genome resequencing analysis identified 7 nonsynonymous mutations of *ppsC* encoding lipopeptide synthetase associated with poly- γ -glutamic acid metabolic pathways. From molecular docking, more binding sites and higher binding energy were speculated between the mutated plipastatin synthase subunit C and glutamate, which might contribute to the higher poly- γ -glutamic acid production. Moreover, the metabolic mechanism analysis revealed that the upregulated amino acids of M32 provided substrates for glutamate and promoted the conversion between L- and D-glutamate acids. In addition, the glycolytic pathway is enhanced, leading to a better capacity for using glucose. The maximum poly- γ -glutamic acid yield of 14.08 g·L⁻¹ was finally reached with 30 g·L⁻¹ glutamate.

Keywords ARTP mutagenesis, *Bacillus licheniformis*, poly- γ -glutamic acid, metabolomics

1 Introduction

Poly- γ -glutamic acid (γ -PGA) is a natural extracellular

Received April 28, 2022; accepted June 14, 2022

E-mails: kelqb@xmu.edu.cn (Li Q.), hening@xmu.edu.cn (He N.)

polymer made up of D-/L-glutamate acid polymerized through γ -glutamyl bonds, mainly synthesized by *Bacillus* sp [1]. Owing to its numerous favourable features, γ -PGA has wide-ranging applications in food, cosmetics, agriculture, medicine, bioremediation, and other industrial fields [1,2]. In recent years, with the in-depth research into γ -PGA synthetic and regulatory mechanisms, several strategies of metabolic engineering have been proposed to enhance γ -PGA production, including strengthening substrate utilization [3], deleting or inhibiting hydrolase genes [4], and increasing energy supply [5,6]. However, the low yield of bacterial γ -PGA is still the main bottleneck at present, which further affects the promotion of γ -PGA application. Therefore, the construction of strains with high γ -PGA yields is important for industrial applications.

Atmospheric and room temperature plasma (ARTP) has been widely used in mutagenesis breeding of bacteria, fungi, and other microorganisms with the advantages of simple operation, high safety, high total mutation rate, and high positive mutation rate [7]. An ARTP mutant *Bacillus coagulans* (*B. coagulans*) GKN316 produced lactic acid at 45.39 g·L⁻¹, which was a 2-fold increase compared to the original strain *B. coagulans* NL01 [8]. A 47.32% enhancement of 1-naphthol was also obtained from *Bacillus cereus* with an ARTP mutation [9]. In addition, without glutamic acid addition, *Bacillus amyloliquefaciens* (*B. amyloliquefaciens*) NX could produce 6.85 g·L⁻¹ γ -PGA. After 90 s of treatment with ARTP, γ -PGA yield was also improved by 58% (10.81 g·L⁻¹) from *B. amyloliquefaciens* NX-2S154 on inulin substrate [10]. Hence, ARTP might be a potential and powerful mutagenesis tool, providing an effective method for obtaining mutants with enhanced γ -PGA yield.

In our previous studies, *Bacillus licheniformis* (*B. licheniformis*) CGMCC (China General Microbiological Culture Collection Center) 2876 was a highly efficient strain producing γ -PGA, and various strategies were adopted to increase its production, including optimizing the medium [11], increasing the supplies of precursors [12], overexpressing key genes [13], and adjusting the regulatory factors. For further enhancement of γ -PGA from the strain, ARTP mutagenesis was adopted, and the underlying mechanism was proposed by means of molecular docking. Genomics and metabolomics analysis provided a complementary demonstration of the metabolic mechanism of the mutant.

2 Experimental

2.1 Cultural conditions

B. licheniformis CGMCC 2876 was obtained from our research group previously [14]. The seed medium for *B. licheniformis* contained the following components: 10 g·L⁻¹ glucose, 0.2 g·L⁻¹ MgSO₄, 0.1 g·L⁻¹ KH₂PO₄, 0.1 g·L⁻¹ K₂HPO₄, 0.1 g·L⁻¹ NaCl, 0.5 g·L⁻¹ urea, and 0.5 g·L⁻¹ yeast extract (pH 7.2). The fermentation medium was 13.9 g·L⁻¹ glucose, 0.048 g·L⁻¹ MgSO₄, 5.6 g·L⁻¹ KH₂PO₄, 1.4 g·L⁻¹ K₂HPO₄, 2 g·L⁻¹ NaCl, 2.67 g·L⁻¹ urea, and 0.6 g·L⁻¹ yeast extract, and the pH was adjusted to 7.2 [15]. Single colonies were cultured in 250 mL conical flasks with 50 mL seed medium for 16 h and then transferred to fermentation medium (4% transfer volume) for 56 h (37 °C, 200 r·min⁻¹). The basic medium for cell growth is Luria–Bertani medium.

2.2 ARTP mutagenesis

B. licheniformis CGMCC 2876 was treated with an ARTP mutagenesis breeding machine. *B. licheniformis* CGMCC 2876 was cultured with Luria–Bertani medium until the logarithmic phase at 37 °C (Fig. 1(a)) and exposed to ARTP mutation for 20, 40, 60, 80, 100, 120, 140, and 160 s, respectively. The main mutagenic parameters of ARTP mutagenesis were as follows: a radio frequency power input of 115 W, 2-mm distance between plasma torch nozzle and sample platform, and a helium gas flow rate of $Q_{He} = 10$ standard litres per minute. Then, the cells were continuously diluted and coated on Luria–Bertani agar to measure mortality. Colonies with wet surfaces and large areas were selected and transferred to seed medium for further study.

2.3 Bacterial screening and characterization

The selection of ARTP strains based on the increased crude γ -PGA production and flocculating activity was

conducted as follows. The crude products were recovered and purified by ethanol precipitation after fermentation. The mixture was centrifuged at 5000 r·min⁻¹ for 5 min to collect sediment. The crude product was freeze-dried to obtain the purified products. As described previously, the flocculating activity was determined by kaolin suspension [12]. The γ -PGA content was measured by high performance liquid chromatography (Agilent Technologies Inc., CA, USA) with an Agilent HC-C18 column (25 cm × 4.6 mm) [13]. Three replicates were set for each experiment. Values are expressed as the mean ± standard deviation, and $p < 0.05$ was used to judge the significant difference among different strains.

2.4 Genome resequencing assay and molecular docking

The DNA of the mutant M32 and *B. licheniformis* CGMCC 2876 was extracted by the sodium dodecyl sulfate method. The whole genome was sequenced using Illumina NovaSeq PE150. The original data obtained by the high-throughput sequencing platform of Illumina PE150 were transformed into raw sequenced reads. The reads were mapped to the reference sequence, and the coverage of the reference sequence to the reads was counted using BWA software V0.7.8 and SAMTOOLS V0.1.18 [16,17].

To further investigate the binding of mutant proteins to substrates, Molecular Operating Environment (MOE) software was applied to molecular docking [18]. The model of PpsC was constructed by SWISS-MODEL, and the stereochemical quality of the models was evaluated. The PpsC model was docked with the substrate by MOE, and the docking scores were negatively correlated with the stability of the bonding.

2.5 Metabolite analysis

The samples in the mid-logarithmic growth phase of fermentation were washed three times with phosphate buffered saline solution. Samples were suspended in 1 mL of extraction solution (methanol, acetonitrile, water volume ratio of 2:2:1). Cell suspensions were treated with ultrasound and then centrifuged to obtain cell metabolites. The bacterial extracts were analysed by liquid chromatography/mass spectrometry (LC/MS) AB Sciex TripleTOF 5600 + (AB Sciex Inc., Singapore, Singapore). 2-Chlorophenylalanine was quantified as an internal standard. The LC/MS data of the identified metabolites of the wild-type strain and the mutant M32 were analysed by SIMCA 14.1 (Umetrics, Umeå, Sweden) [19].

2.6 Quantitative real-time polymerase chain reaction (qRT-PCR) analysis

Total RNA and complementary DNA were collected from

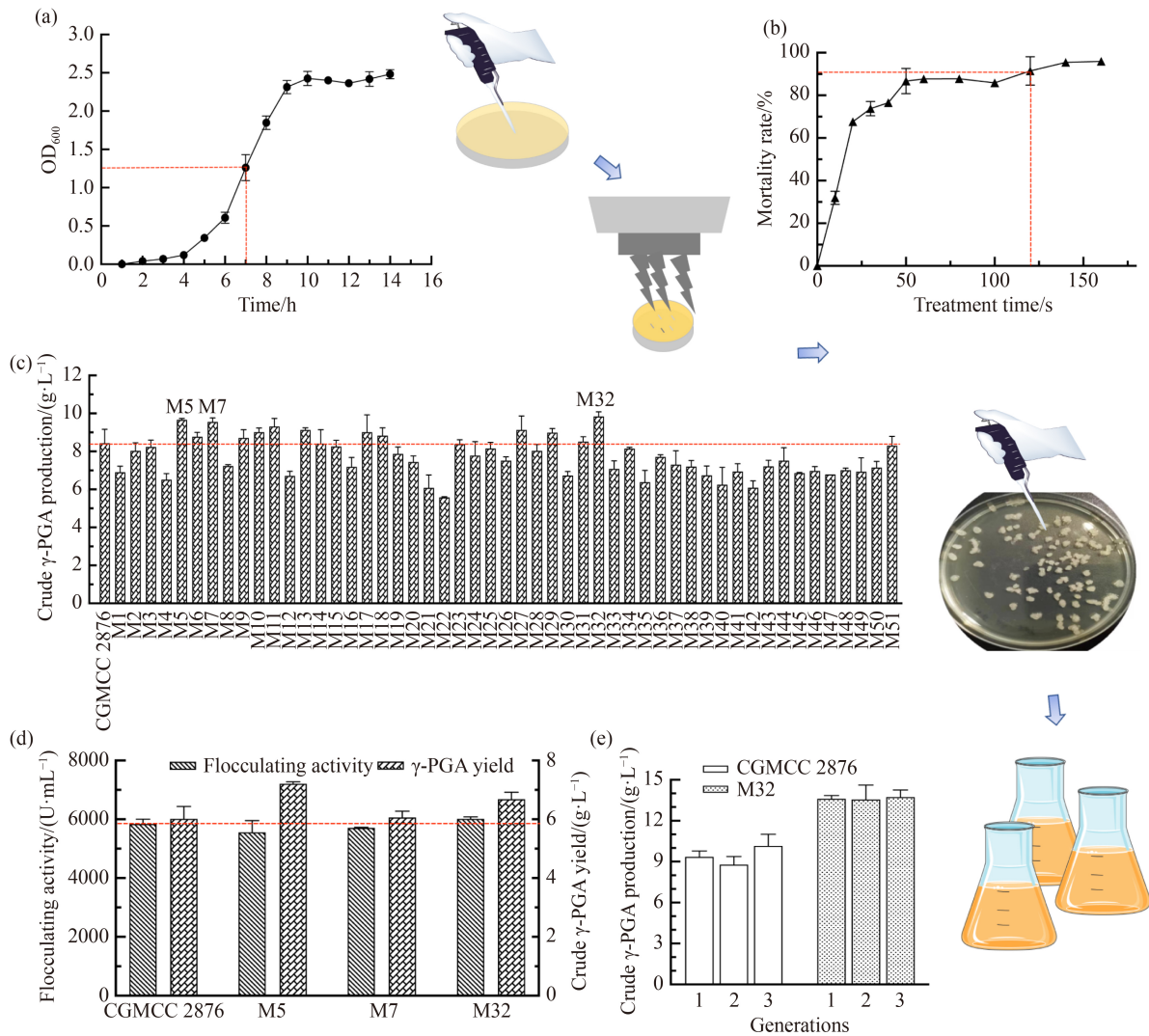


Fig. 1 ARTP mutagenesis and characteristics of screened *B. licheniformis*. (a) Growth curve of *B. licheniformis* CGMCC 2876; (b) Effects of ARTP treatment time on the mortality rate of *B. licheniformis*; (c) Analysis of the crude γ -PGA yield of ARTP-mutated strains; (d) γ -PGA production and flocculating activity of the rescreened strains; (e) The stability of the mutant M32.

B. licheniformis CGMCC 2876 and mutant M32 after 24 h of incubation. The qTOWER3 instrument (Analytik Jena, Germany) was used to detect the differential expression of target genes. The reference gene was 16S rRNA in the calculations, and the related primers are listed in Appendix A.

3 Results and discussion

3.1 Breeding a performance improvement of *B. licheniformis* by ARTP mutagenesis

The process of induction and screening of *B. licheniformis* through ARTP mutagenesis is shown in Fig. 1. We determined the logarithmic phase of the OD₆₀₀ (optical density measured at a wavelength of 600 nm) value between 1.25 and 1.5 to ensure that the *B.*

licheniformis CGMCC 2876 culture was in the optimal treatment period (Fig. 1(a)). According to Fig. 1(b), the mortality rate of the strain reached 100% when treated with ARTP for 160 s. The positive mutation rate has been demonstrated to be the highest when the mortality rate of mutation was over 95% [20]. Therefore, 120 s was identified as the optimal treatment time (Fig. 1(b)).

Among the 51 ARTP-mutated strains (Fig. 1(c)), we obtained 3 mutant isolates with increased crude γ -PGA production, including M5 (9.66 $\text{g}\cdot\text{L}^{-1}$), M7 (9.55 $\text{g}\cdot\text{L}^{-1}$), and M32 (9.87 $\text{g}\cdot\text{L}^{-1}$). M32 exhibited a significant increase in flocculating activity (6017 $\text{U}\cdot\text{mL}^{-1}$) and γ -PGA production (6.68 $\text{g}\cdot\text{L}^{-1}$) compared with *B. licheniformis* CGMCC 2876 (Fig. 1(d)). Furthermore, M32 exhibited better genetic stability (Fig. 1(e)).

For the mutant M32, the crude extracellular polymer yield reached 13.6 $\text{g}\cdot\text{L}^{-1}$, among which γ -PGA reached $6.68 \pm 0.35 \text{ g}\cdot\text{L}^{-1}$, which was 11% higher than γ -PGA yield of *B. licheniformis* CGMCC 2876 (Table 1).

Table 1 Productions and compositions of extracellular polymers produced by *B. licheniformis* CGMCC 2876 and the mutant M32

Characters	CGMCC 2876	M32
Crude yield/(g·L ⁻¹)	9.36 ± 0.24	13.6 ± 0.26
γ-PGA/(g·L ⁻¹)	6.01 ± 0.34	6.68 ± 0.35
Total sugar/(g·L ⁻¹)	0.35 ± 0.02	0.35 ± 0.04
Protein/(g·L ⁻¹)	0.15 ± 0.05	0.15 ± 0.05
Other components/(g·L ⁻¹)	4.33 ± 0.12	6.42 ± 0.15

However, the yield of exopolysaccharide and protein did not show a significant increase after ARTP mutagenesis. Other components of the extracellular polymer of M32 improved from 4.33 to 6.42 g·L⁻¹, including nucleic acids, lipoproteins, glycoproteins, etc.

3.2 Genomics analysis

Generally, ARTP could induce unique and positive genetic responses, so stable mutants are produced through ARTP [21,22]. By comparative genomics, 54 single nucleotide polymorphisms (SNPs) and 7 insertion/deletions (InDels) of the mutant M32 were detected. Thirty-three SNPs were located in the intergenic regions, and 21 SNPs (Table 2) were in the coding sequence, including 18 nonsynonymous SNPs and 3 synonymous SNPs. Meanwhile, 7 InDels were detected in M32 in the intergenic regions. Therefore, the InDels did not alter the sequence of the gene coding region. In addition, M32 had an intrachromosomal translocation, which was approximately 273 bp in length.

As shown in Table 2, 6 genes were mutated after ARTP mutagenesis in the mutant M32. Seven nonsynonymous SNPs were detected in *ppsC* encoding plipastatin synthase subunit C (PpsC). A synonymous SNP was detected in *ppsC_1*, and a nonsynonymous SNP was detected in *ppsA*, which was homologous to *ppsC*. *ppsC*, *ppsA_1*, and *ppsC_1* are subunits of the lipopeptide antibiotic plipastatin synthase, which is a multifunctional enzyme capable of polymerizing amino acids into short peptide chains containing glutamate [23,24]. We speculate that the mutation of *ppsC* may be positively correlated with the increased yields of γ-PGA. In addition, the *rnjA*-encoded ribonuclease J1 had a nonsynonymous SNP. The *grsA* gene had 2 nonsynonymous SNPs, and *grsA* is involved in the antibiotic Gramicidin S biosynthetic pathway [25]. A synonymous SNP and 7 nonsynonymous SNPs occurred

in *lgrB*, which was subunit B of linear synthase. This enzyme activated the 3rd to 6th amino acids in linear graminotin, catalysing the formation of peptide bonds between them [26].

Molecular docking was further applied to explore the binding effect of the PpsC protein with its substrate with MOE software in Fig. 2. Previous studies have shown that PpsC can accelerate the activation and polymerization of glutamate (Glu), valine (Val), and alanine (Ala) [27]. In the synthesis of the lipopeptide antibiotic plipastatin, there were competitive sites for glutamate, valine, and alanine. In *B. licheniformis* CGMCC 2876, there were 4 binding sites between PpsC and glutamate, among which there was a hydrogen bond with Asp1886, two hydrogen bonds with Arg1976, and one hydrogen bond with Arg1975 (Fig. 2(a)). After ARTP mutagenesis, PpsC had 5 binding sites with glutamate: two hydrogen bonds with Asp1868, one hydrogen bond with Lys1972, and two hydrogen bonds with Arg1883. The hydrogen bonds with Arg1975 and Arg1976 disappeared, and the free binding energy of PpsC with glutamic acid was increased from -15.3 to -18.2 kcal·mol⁻¹ (Table 3). Compared to glutamic acid, PpsC of mutant M32 showed different binding states with valine and alanine. In the wild-type *B. licheniformis* CGMCC 2876, there were 5 binding sites between PpsC and valin, while only 3 binding sites existed after mutation (Fig. 2(b)). With the disappearance of the hydrogen bond with tyrosine, the binding free energy of PpsC to valine decreased from -15.2 to -11.1 kcal·mol⁻¹ (Table 3). The reduction in the number of alanine binding sites in PpsC was similar to the reduction in the number of binding sites with valine (Fig. 2(c)). Before ARTP mutagenesis, PpsC had 5 binding sites, two hydrogen bonds with Asp1868 and Arg1883, and one hydrogen bond with Tyr1779. While PpsC and alanine had 3 binding sites in the mutant M32, 1 hydrogen bond with Lys1972, Tyr1880 and Asp1868. The binding free energy of PpsC with alanine decreased from -15.2 to -11.1 kcal·mol⁻¹ (Table 3).

In conclusion, the mutant PpsC had a higher binding energy and more binding sites for glutamate, while the mutant PpsC had fewer binding sites for valine and alanine, and the binding energy decreased. Glutamate is a key amino acid in the synthesis of the lipopeptide plipastatin [28,29], so the enhanced binding of PpsC to glutamate may promote the synthesis of lipopeptides.

Table 2 SNPs analysis of M32

Gene	Definition	Amino acid change
<i>ppsC_1</i>	Plipastatin synthase subunit C	Phe1266Phe
<i>ppsA_1</i>	Plipastatin synthase subunit A	Arg29Ser
<i>ppsC</i>	Plipastatin synthase subunit C	Arg1092Cys, Val1250Met, Ala915Met, Tyr963Tyr, Ala1117Ser, Tyr926His, Ala931Tyr, Gln4652His
<i>rnjA</i>	Ribonuclease J1	Leu477Thr
<i>grsA</i>	Gramicidin S synthase 1	Pro20Ala, Ala26Ser
<i>lgrB</i>	Antiholin-like protein	Asp4656Gln, His154Arg, Thr4661Ala, Arg4651Arg, Asp4658His, Gly160Glu, Thr4661Ala, Ser4647Ile

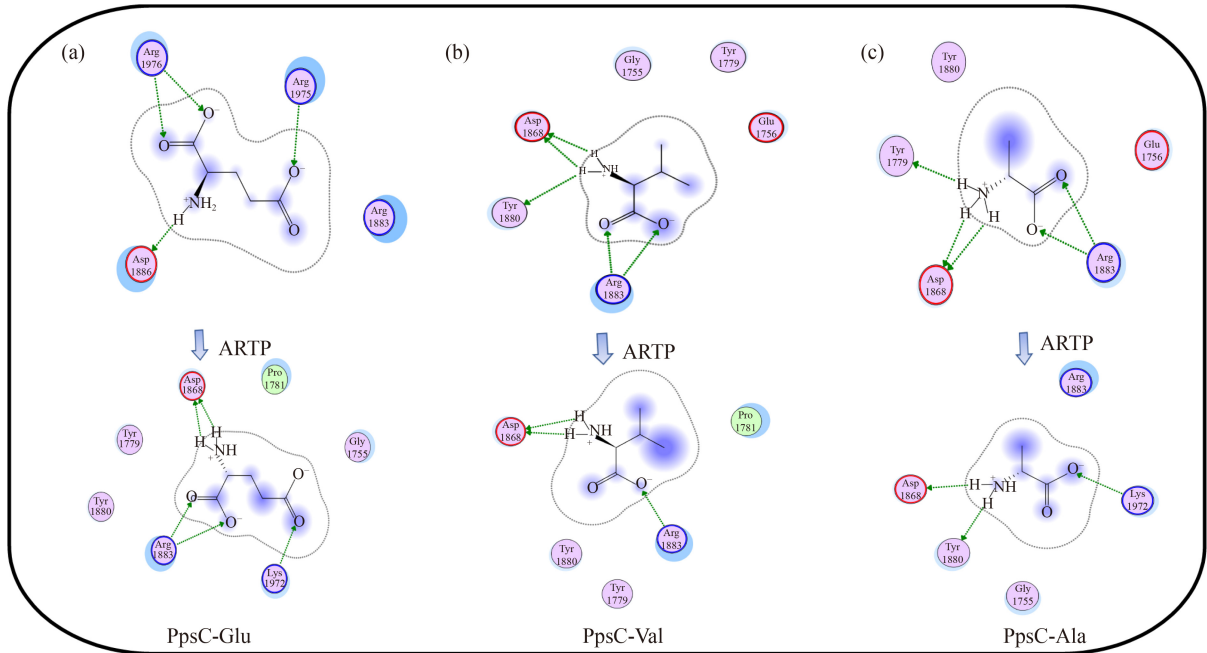


Fig. 2 The molecular simulation docking of PpsC and (a) glutamate, (b) valine and (c) alanine before and after ARTP mutagenesis in *B. licheniformis* CGMCC 2876 (up) and the mutant M32 (down).

Table 3 The PpsC docking score and the key amino acids combined with the ligands in *B. licheniformis* CGMCC 2876 and the mutant M32

Strain	Substrate	Score/ (kcal·mol ⁻¹)	Bound amino acid
<i>B. licheniformis</i> CGMCC 2876	Glu	-15.3	Asp1886, Arg1976, Arg1975
	Val	-14.9	Arg1883, Asp1868
	Ala	-15.2	Asp1868, Tyr1880, Arg1883
M32	Glu	-18.2	Asp1868, Lys1972, Arg1883
	Val	-11.5	Arg1883, Asp1868
	Ala	-11.1	Asp1868, Lys1972

Previous studies have shown that exogenous addition of 3 mg·L⁻¹ lipopeptides can significantly improve γ -PGA production up to 17.9% of *B. licheniformis*, and the increase in lipopeptide leads to the transfer of carbon flux to glutamate and γ -PGA synthesis pathways through the tricarboxylic acid (TCA) cycle [30]. Thus, the variation in PpsC may be responsible for the enhancement of γ -PGA yield.

3.3 Metabonomic analysis

To further investigate metabolic changes in M32 (Fig. 3), LC/MS combined with multivariate analysis was used. A total of over 140 intracellular metabolites were analysed, and principal component analysis (PCA, Fig. 3(a)) and orthogonal partial least squares discriminant analysis (OPLS-DA, Fig. 3(b)) were constructed, which showed remarkable separation of metabolites and the significant diversity of the metabolic profiles between *B. licheniformis* CGMCC 2876 and the mutant M32. Differential metabolites ($VIP > 1$, $P < 0.05$) of *B. licheniformis* CGMCC 2876 and the mutant M32 are

visually shown in the heatmap plot (Fig. 3(c)) [31].

To analyse the overview of differential metabolomics, the metabolomics network was constructed and visually displayed (Fig. 4). The metabolites of mutant M32 are involved in the TCA cycle, glycolysis pathway and amino acid metabolism pathway. The metabolites of glucose-6-phosphate (G-6-P) and fructose-6-phosphate (F-6-P) in the glycolytic pathway after mutation were significantly increased by 13 times, indicating that M32 can better use glucose to provide more carbon sources for γ -PGA synthesis. However, there was no significant change in α -ketoglutaric acid and glutamic acid after ARTP mutagenesis in M32, possibly because glutamate-independent *B. licheniformis* tends to be stable in the carbon metabolism pathway in culture conditions without glutamic acid [32]. Since glutamate is more commonly used in the synthesis of proline and arginine, proline and arginine were increased in M32. The presence of amino acids can influence lipopeptide production [33]. For example, exogenous proline can enhance the lipopeptide production of *B. amyloliquefaciens* HM618 [34]. Thus, combined with the enhancement of binding between PpsC and glutamate, proline and arginine may promote the synthesis of lipopeptides, which leads to increased γ -PGA production.

Notably, alanine in M32 was upregulated 3.5 times. The increase in phosphoenolpyruvate in the mutant M32 contributed to the increase in pyruvate, a precursor of alanine. Meanwhile, the decreased binding ability of alanine to PpsC in M32 resulted in the accumulation of alanine. In addition, alanine is an intermediate of D- and L-glutamate acid [35], and γ -PGA is synthesized by D-/L-

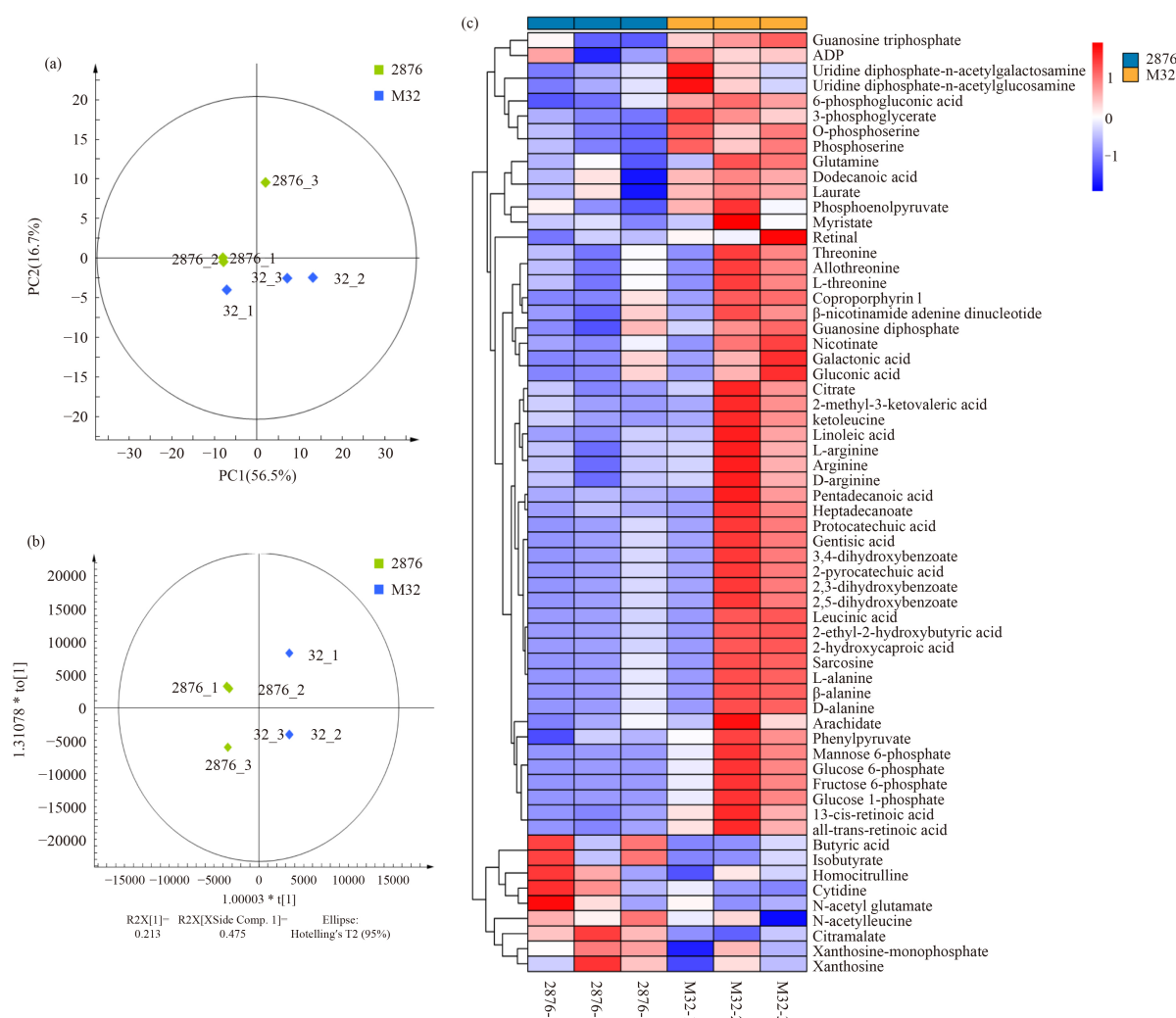


Fig. 3 Comparative metabolomic analysis of *B. licheniformis* CGMCC 2876 and the mutant M32. (a) The PCA score plot and (b) OPLS-DA score plot were obtained between *B. licheniformis* CGMCC 2876 and M32. (c) Heatmap of 60 differential metabolites for normalized concentrations. The normalized abundance values are indicated from blue (increase) to red (decrease).

glutamate acid through polyglutamic acid synthase. L-Glutamic acid is synthesized via L-glutamic pyruvate transaminase, then converted to D-alanine through alanine racemase, and finally converted to D-glutamic acid under the action of D-glutamic pyruvate transaminase [36]. Hence, on one hand, the upregulation of alanine stimulated the TCA cycle, which facilitated the synthesis of glutamate from α-ketoglutaric acid. On the other hand, the accumulation of alanine also promoted the transformation of L-glutamate and D-glutamate, which ultimately led to the enhancement of γ-PGA production.

Moreover, phenylalanine and aspartic acid were also upregulated. Zhang et al. [37] added 3 g·L⁻¹ aspartic acid and 1.5 g·L⁻¹ phenylalanine, and the production of γ-PGA improved by 23.18% and 12.15%, respectively, indicating that phenylalanine and aspartic acid promoted the production of γ-PGA. Aspartic acid is transformed from oxaloacetic acid and glutamate, and aspartic acid can be transformed into glutamate under the action of glutamic-oxalacetic transaminase [38]. Thus, the

enhancement of phenylalanine and aspartic acid was beneficial to the synthesis of γ-PGA to provide more substrates, resulting from the transformation to glutamate [39]. In addition, serine in mutant M32 was increased, and the expression of pyruvate kinase (*pyk*) was also increased due to the activation of serine [40], while phosphoenolpyruvate, the substrate of *pyk*, was increased 1.6 times. Pyruvate is the metabolite most associated with the TCA cycle [41]. Additionally, glutamine in the mutant M32 was increased 1.7 times, and the concentration of glutamine is closely related to the amount of glutamate required [42].

3.4 Analysis of the expression levels of key genes

qRT-PCR was used to analyse the expression levels of key genes in the γ-PGA synthesis pathway (Fig. 5). The γ-PGA synthetase complex system CapBCA is encoded by *capA*, *capB*, and *capC* [36]. The results indicated that the expression of the *capA*, *capB*, and *capC* genes of the

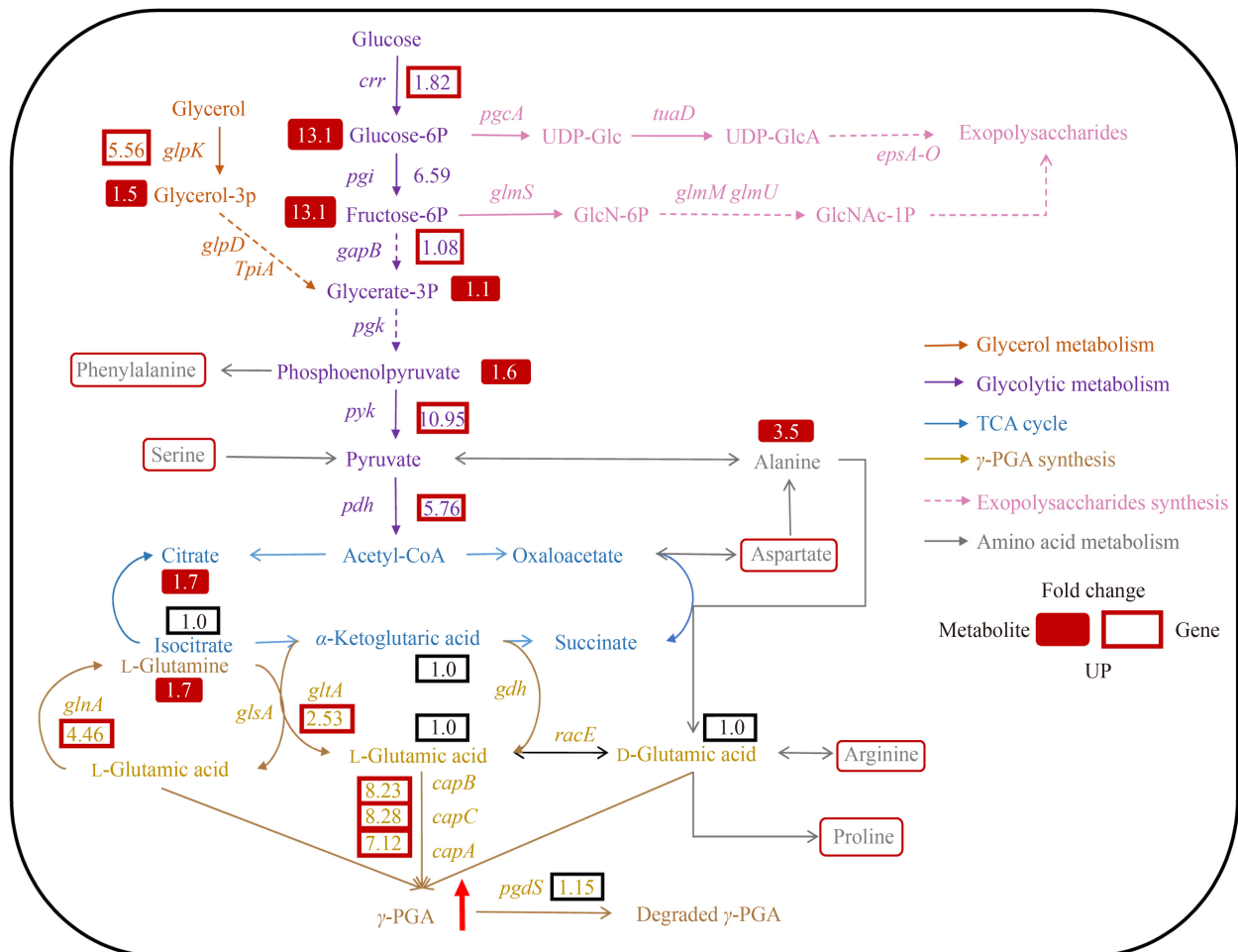


Fig. 4 The intracellular metabolites and key genes in the γ -PGA synthetic pathways in *B. licheniformis* CGMCC 2876 and the mutant M32. The number represents the multiple of the M32 mutant compared to the wild-type strain.

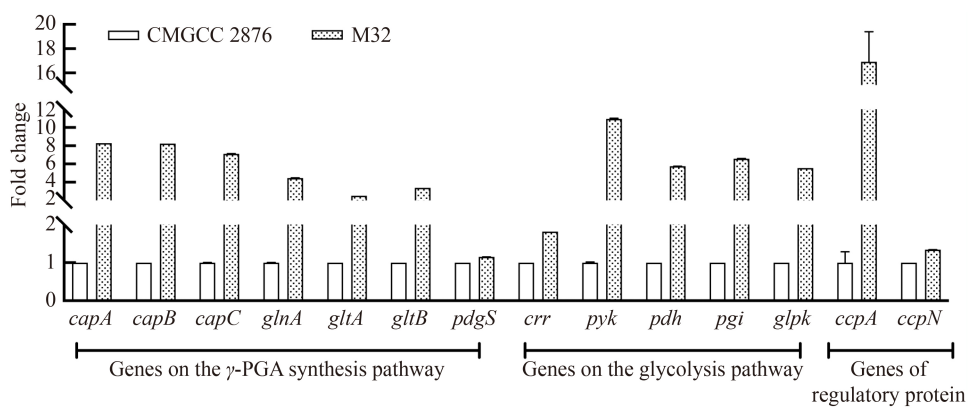


Fig. 5 Gene expression in the γ -PGA synthesis and glycolysis pathways of *B. licheniformis* CGMCC 2876 and the mutant M32.

mutant M32 was upregulated by 8.28, 8.23, and 7.12 times, respectively, while *pgdS* did not change significantly. In *B. amyloliquefaciens*, *pgdS* has been shown to hydrolyse γ -PGA, resulting in a reduction in γ -PGA yield [43]. In addition, the expression levels of *gltA* and *gltB*, which encode glutamate synthetase, were upregulated by 2.53 times and 3.4 times, respectively, in the mutant M32.

Analysis of the expression levels of genes in the glycolysis pathway revealed that ARTP mutagenesis also resulted in the upregulation of *crr*, *pyk*, *pdh*, *pgi*, and *glpk* (Fig. 5). Encoding G-6-P isomerase, *pgi* was upregulated by 6.59 times. Fructose is responsible for catalysing the conversion of G-6-P to F-6-P to promote glucose utilization by cells through glycolysis [44]. Moreover, encoding *pyk*, *pyk* was upregulated by 10.95 times, which

catalysed the conversion of phosphoenolpyruvate to pyruvate and generated adenosine triphosphate [45]. Metabolomics data indicated that phosphoenolpyruvate was upregulated; thus, the upregulation of *pyk* promoted pyruvate production, and pyruvate also provided a precursor for the TCA cycle and glutamate. The expression of *pdh* (pyruvate dehydrogenase) was upregulated by 5.76 times, improving the acetyl-CoA supply for the TCA cycle, which may be beneficial to the synthesis of γ -PGA.

In addition, the expression of *ccpA*, encoding the carbon metabolism regulatory protein CcpA, was upregulated by 16.93 times in the mutant M32, while the expression of the gene *ccpN*, encoding the metabolic regulatory protein CcpN, did not change significantly (Fig. 5). In the presence of excess glucose, the TCA cycle is inhibited by a CcpA-dependent catabolite repression mechanism [46]. CcpA acted mainly on the growth of microbial cells and the synthesis of extracellular polymers. As glucose is exhausted, CcpA activates glutamate synthase (GltAB) and inhibits the expression of amine dehydrogenase [47]. The expression of *ccpA* in the mutant strain was upregulated, which promoted the upregulation of *gltAB* expression and ultimately increased the yield of γ -PGA.

3.5 Performance of sodium glutamate utilization

According to the foregoing analysis, M32 could better utilize glutamate to accumulate a higher γ -PGA yield. Thus, we explored the effects of supplemental different levels of sodium glutamate in the culture medium on γ -PGA production from *B. licheniformis* CGMCC 2876 and the mutant M32 (Fig. 6). As expected, the γ -PGA yield of M32 was significantly higher than that of *B. licheniformis* CGMCC 2876 with all concentration of exogenous sodium glutamate. In particular, the γ -PGA yield of the mutated strain M32 reached 14.08 g·L⁻¹ in sodium glutamate (30 g·L⁻¹) medium, which was much higher than the γ -PGA yield of *B. licheniformis* CGMCC

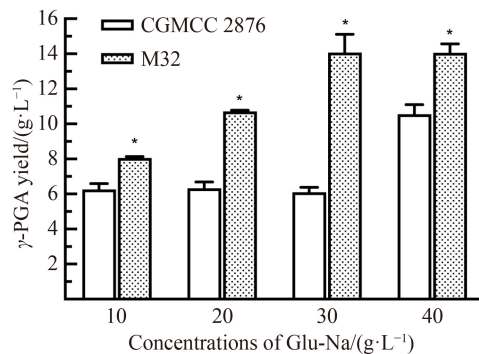


Fig. 6 Effects of sodium glutamate supplementation on γ -PGA yields of *B. licheniformis* CGMCC 2876 and the mutant M32. The single asterisks indicate significant differences in each group ($P < 0.05$).

2876 (6.1 g·L⁻¹). These results proved that M32 had a stronger absorption and utilization capacity for glutamate sodium.

4 Conclusions

In this study, *B. licheniformis* CGMCC 2876 was treated by ARTP mutagenesis to obtain *B. licheniformis* with high γ -PGA production. The yield of γ -PGA in mutant M32 was 6.68 g·L⁻¹, which was 11% higher than the γ -PGA yield of the original strain. Seven SNPs were detected in *ppcC* by genome resequencing. The mutated PpsC possessed more binding sites and a higher binding energy with glutamate according to molecular docking simulation, which may promote the synthesis of the lipopeptide plipastatin. By comparing metabolomics, the upregulated metabolite alanine of the mutant strain was found to stimulate TCA to synthesize glutamate and promoted the conversion between L- and D-glutamate acids. Proline and arginine may promote the synthesis of lipopeptides, thus increasing the γ -PGA yield. In addition, the glycolytic pathway was enhanced, leading to a better capacity for using glucose. The expression levels of *capA*, *capB*, and *capC* were upregulated accordingly. A maximum γ -PGA yield of 14.08 g·L⁻¹ was finally reached with 30 g·L⁻¹ glutamate. This work provides theoretical support for the synthesis mechanism of γ -PGA in *B. licheniformis* and provides a method for obtaining potential strains with high γ -PGA industrial production.

Acknowledgements This work was financially supported by the National Natural Science Foundation of China (Grant Nos. 32170061 and 31871779).

Appendix A Primers used in qRT-PCR in this experiment

Gene	Primer sequence (5' to 3')
q- <i>crr</i> -F	TCAAGCCGCATCCACC
q- <i>crr</i> -R	AAGTTCTCCAATAAAATCTCC
q- <i>pyk</i> -F	CAGCCGCTTTCAAGGGAC
q- <i>pyk</i> -R	CAGCCGCTTTCAAGGGAC
q- <i>pdh</i> -F	CTCTTGTCTTGGTGCGGGGA
q- <i>pdh</i> -R	CATTCTCATAGCGGTGGCCT
q- <i>pgi</i> -F	CTTCGGCAGCACATTG
q- <i>pgi</i> -R	GTCGCCAACCATACCAT
q- <i>glpk</i> -F	GCGTGCCTAACCTACAAA
q- <i>glpk</i> -R	CGTGATGGGCTGAGAATG
q- <i>gapB</i> -F	ACGCTGGAGACGATTGC
q- <i>gapB</i> -R	CCACGGAAGAAGTTAGGG
q- <i>capA</i> -F	CCATTGCGAAGGAGTT
q- <i>capA</i> -R	GCTGACGAACGCAGGAGAA
q- <i>capB</i> -F	GAATTGTCTGCCACGATGACT
q- <i>capB</i> -R	GATGGGACCGACTTTGGAT
q- <i>capC</i> -F	AGCGTAATCGTTAATCCCTGTC
q- <i>capC</i> -R	CGGTGATGCCGTTGAGA
q- <i>glnA</i> -F	AGTCATGGTCAAAGCCCTCG
q- <i>glnA</i> -R	CTCCAAGGGTGGACTTGTG
q- <i>gltA</i> -F	GGCAACAAAGTGTATCC

(Continued)

Gene	Primer sequence (5' to 3')
q-gltA-R	TCGGTGAGGCTCCAGTG
q-gltB-F	AGCGTCGCCAGTTCCGG
q-gltB-R	CGCCTCTTCATAAGCATAGT
q-pdgS-R	AGACATCTGAGGGTGC
q-pdgS-R	TCCGTTGATTTGTGCTG
q-ccpN-F	CCTGTTGCCGATGCTG
q-ccpN-R	CGGGGTCGGTTATTTC
q-ccpA-F	CGAGCCGTAAGGAACA
q-ccpA-R	GCTTGCCATTGAGGAA
q-16S-F	CAGATTGTGGATTGGCTTAG
q-16S-R	CGTGTGAGATGTTGGGT

References

1. Li D, Hou L, Gao Y, Tian Z, Fan B, Wang F, Li S. Recent advances in microbial synthesis of poly- γ -glutamic acid: a review. *Foods*, 2022, 11(5): 1–19
2. Cao M, Feng J, Sirisansaneeyakul S, Song C, Chisti Y. Genetic and metabolic engineering for microbial production of poly- γ -glutamic acid. *Biotechnology Advances*, 2018, 36(5): 1424–1433
3. Zhan Y Y, Zhu C J, Sheng B J, Cai D B, Wang Q, Wen Z Y, Chen S W. Improvement of glycerol catabolism in *Bacillus licheniformis* for production of poly- γ -glutamic acid. *Applied Microbiology and Biotechnology*, 2017, 101(19): 7155–7164
4. Tian G, Fu J, Wei X, Ji Z, Ma X, Qi G, Chen S. Enhanced expression of *pgdS* gene for high production of poly- γ -glutamic acid with lower molecular weight in *Bacillus licheniformis* WX-02. *Journal of Chemical Technology and Biotechnology* (Oxford, Oxfordshire), 2014, 89(12): 1825–1832
5. Li B C, Cai D B, Hu S Y, Zhu A T, He Z L, Chen S W. Enhanced synthesis of poly gamma glutamic acid by increasing the intracellular reactive oxygen species in the *Bacillus licheniformis* 1-pyrroline-5-carboxylate dehydrogenase gene *ycgN*-deficient strain. *Applied Microbiology and Biotechnology*, 2018, 102(23): 10127–10137
6. Cai D B, Chen Y Z, He P H, Wang S Y, Mo F, Li X, Wang Q, Nomura C T, Wen Z Y, Ma X, Chen S. Enhanced production of poly- γ -glutamic acid by improving ATP supply in metabolically engineered *Bacillus licheniformis*. *Biotechnology and Bioengineering*, 2018, 115(10): 2541–2553
7. Ottenheim C, Nawrath M, Wu J C. Microbial mutagenesis by atmospheric and room-temperature plasma (ARTP): the latest development. *Bioresources and Bioprocessing*, 2018, 5(12): 1–12
8. Jiang T, Qiao H, Zheng Z J, Chu Q L, Li X, Yong Q, Ouyang J. Lactic acid production from pretreated hydrolysates of corn stover by a newly developed *Bacillus coagulans* strain. *PLoS One*, 2016, 11(2): e0149101
9. Qiu C G, Zhang A, Tao S, Li K, Chen K Q, Ouyang P K. Combination of ARTP mutagenesis and color-mediated high-throughput screening to enhance 1-naphthol yield from microbial oxidation of naphthalene in aqueous system. *Frontiers of Chemical Science and Engineering*, 2020, 14(5): 793–801
10. Qiu Y B, Zhang Y T, Zhu Y F, Sha Y Y, Xu Z Q, Feng X H, Li S, Xu H. Improving poly-(γ -glutamic acid) production from a glutamic acid-independent strain from inulin substrate by consolidated bioprocessing. *Bioprocess and Biosystems Engineering*, 2019, 42(10): 1711–1720
11. Yu W, Chen Z, Ye H, Liu P, Li Z, Wang Y, Li Q, Yan S, Zhong C J, He N. Effect of glucose on poly- γ -glutamic acid metabolism in *Bacillus licheniformis*. *Microbial Cell Factories*, 2017, 16(1): 22
12. Chen Z, Liu P, Li Z, Yu W, Wang Z, Yao H, Wang Y, Li Q, Deng X, He N. Identification of key genes involved in polysaccharide bioflocculant synthesis in *Bacillus licheniformis*. *Biotechnology and Bioengineering*, 2017, 114(3): 645–655
13. Liu P, Chen Z, Yang L, Li Q, He N. Increasing the bioflocculant production and identifying the effect of overexpressing *epsB* on the synthesis of polysaccharide and γ -PGA in *Bacillus licheniformis*. *Microbial Cell Factories*, 2017, 16(1): 163
14. Xiong Y, Wang Y, Yu Y, Li Q, Wang H, Chen R, He N. Production and characterization of a novel bioflocculant from *Bacillus licheniformis*. *Applied and Environmental Microbiology*, 2010, 76(9): 2778–2782
15. Chen Z, Meng T, Li Z, Liu P, Wang Y, He N, Liang D. Characterization of a beta-glucosidase from *Bacillus licheniformis* and its effect on bioflocculant degradation. *AMB Express*, 2017, 7(1): 197
16. Li H, Durbin R. Fast and accurate short read alignment with Burrows–Wheeler transform. *Bioinformatics* (Oxford, England), 2009, 25(14): 1754–1760
17. Li H, Handsaker B, Wysoker A, Fennell T, Ruan J, Homer N, Marth G, Abecasis G, Durbin R. Genome Project Data P. The sequence alignment/map format and SAMtools. *Bioinformatics* (Oxford, England), 2009, 25(16): 2078–2079
18. Rahim F, Ullah H, Javid M T, Wadood A, Taha M, Ashraf M, Shaukat A, Junaid M, Hussain S, Rehman W, Mehmood R, Sajid M, Khan M N, Khan K M. Synthesis, *in vitro* evaluation and molecular docking studies of thiazole derivatives as new inhibitors of α -glucosidase. *Bioorganic Chemistry*, 2015, 62: 15–21
19. Sadiq F A, Yan B W, Zhao J X, Zhang H, Chen W. Untargeted metabolomics reveals metabolic state of *Bifidobacterium bifidum* in the biofilm and planktonic states. *LWT*, 2020, 118: 108772–108779
20. Cao S, Zhou X, Jin W B, Wang F, Tu R J, Han S F, Chen H Y, Chen C, Xie G J, Ma F. Improving of lipid productivity of the oleaginous microalgae *Chlorella pyrenoidosa* via atmospheric and room temperature plasma (ARTP). *Bioresource Technology*, 2017, 244: 1400–1406
21. Fang M Y, Jin L H, Zhang C, Tan Y Y, Jiang P X, Ge N, Li H P, Xing X H. Rapid mutation of *Spirulina platensis* by a new mutagenesis system of atmospheric and room temperature plasmas (ARTP) and generation of a mutant library with diverse phenotypes. *PLoS One*, 2013, 8(10): e77046
22. Wang L Y, Huang Z L, Li G, Zhao H X, Xing X H, Sun W T, Li H P, Gou Z X, Bao C Y. Novel mutation breeding method for *Streptomyces avermitilis* using an atmospheric pressure glow discharge plasma. *Journal of Applied Microbiology*, 2010, 108(3): 851–858
23. Lilge L, Vahidinasab M, Adiek I, Becker P, Nesamani C K,

- Treinen C, Hoffmann M, Heravi K M, Henkel M, Hausmann R. Expression of *degQ* gene and its effect on lipopeptide production as well as formation of secretory proteases in *Bacillus subtilis* strains. *MicrobiologyOpen*, 2021, 10(5): 1–10
24. Tsuge K, Ano T, Hirai M, Nakamura Y, Shoda M. The genes *degQ*, *pps*, and *lpa-8 (sfp)* are responsible for conversion of *Bacillus subtilis* 168 to plipastatin production. *Antimicrobial Agents and Chemotherapy*, 1999, 43(9): 2183–2192
25. Stein T, Kluge B, Vater J, Franke P, Otto A, Wittmannliebold B. Gramicidin-S synthetase-1 (phenylalanine racemase), a prototype of amino-acid racemases containing the cofactor 4'-phosphopantetheine. *Biochemistry*, 1995, 34(14): 4633–4642
26. Bu X Z, Wu X M, Ng N L J, Mak C K, Qin C G, Guo Z H. Synthesis of gramicidin S and its analogues via an on-resin macrolactamization assisted by a predisposed conformation of the linear precursors. *Journal of Organic Chemistry*, 2004, 69(8): 2681–2685
27. Liu H X, Gao L, Han J Z, Ma Z, Lu Z X, Dai C, Zhang C, Bie X M. Biocombinatorial synthesis of novel lipopeptides by COM domain-mediated reprogramming of the plipastatin NRPS complex. *Frontiers in Microbiology*, 2016, 7: 1801
28. Heinzelmann E, Berger S, Puk O, Reichenstein B, Wohlleben W, Schwartz D. A glutamate mutase is involved in the biosynthesis of the lipopeptide antibiotic friulimicin in *Actinoplanes friuliensis*. *Antimicrobial Agents and Chemotherapy*, 2003, 47(2): 447–457
29. Wang J Q, Guo R J, Wang W C, Ma G Z, Li S D. Insight into the surfactin production of *Bacillus velezensis* B006 through metabolomics analysis. *Journal of Industrial Microbiology & Biotechnology*, 2018, 45(12): 1033–1044
30. Qiu Y M, Wang Q, Zhu C J, Yang Q Q, Zhou S Y, Xiang Z W, Chen S W. Deciphering metabolic responses of biosurfactant lichenysin on biosynthesis of poly-glutamic acid. *Applied Microbiology and Biotechnology*, 2019, 103(10): 4003–4015
31. Farres M, Platikanov S, Tsakovski S, Tauler R. Comparison of the variable importance in projection (VIP) and of the selectivity ratio (SR) methods for variable selection and interpretation. *Journal of Chemometrics*, 2015, 29(10): 528–536
32. Halmschlag B, Putri S P, Fukusaki E, Blank L M. Identification of key metabolites in poly- γ -glutamic acid production by tuning γ -PGA synthetase expression. *Frontiers in Bioengineering and Biotechnology*, 2020, 8: 1–14
33. Wu J Y, Liao J H, Shieh C J, Hsieh F C, Liu Y C. Kinetic analysis on precursors for iturin A production from *Bacillus amyloliquefaciens* BPD1. *Journal of Bioscience and Bioengineering*, 2018, 126(5): 630–635
34. Chen X Y, Sun H Z, Qiao B, Miao C H, Hou Z J, Xu S J, Xu Q M, Cheng J S. Improved the lipopeptide production of *Bacillus amyloliquefaciens* HM618 under co-culture with the recombinant *Corynebacterium glutamicum* producing high-level proline. *Bioresouce Technology*, 2022, 349: 126863
35. Klenchin V A, Schmidt D M, Gerlt J A, Rayment I. Evolution of enzymatic activities in the enolase superfamily: structure of a substrate-ligated complex of the L-Ala-D/L-Glu epimerase from *Bacillus subtilis*. *Biochemistry*, 2004, 43(32): 10370–10378
36. Xu G Q, Zha J, Cheng H, Ibrahim M H A, Yang F, Dalton H, Cao R, Zhu Y X, Fang J H, Chi K J, Zheng P, Zhang X, Shi J, Xu Z, Gross R A, Koffas M A G. Engineering *Corynebacterium glutamicum* for the de novo biosynthesis of tailored poly- γ -glutamic acid. *Metabolic Engineering*, 2019, 56: 39–49
37. Zhang C, Wu D J, Qiu X L. Stimulatory effects of amino acids on γ -polyglutamic acid production by *Bacillus subtilis*. *Scientific Reports*, 2018, 8(1): 1–9
38. Niu D D, Li C Y, Wang P, Huang L, McHunu N P, Singh S, Prior B A, Ye X Y. Twin-arginine signal peptide of *Bacillus licheniformis* GlmU efficiently mediated secretory expression of protein glutaminase. *Electronic Journal of Biotechnology*, 2019, 42: 49–55
39. Zhang Q, Chen Y Z, Gao L, Chen J G, Ma X, Cai D B, Wang D, Chen S W. Enhanced production of poly- γ -glutamic acid via optimizing the expression cassette of *Vitreoscilla hemoglobin* in *Bacillus licheniformis*. *Synthetic and Systems Biotechnology*, 2022, 7(1): 567–573
40. Chaneton B, Hillmann P, Zheng L, Martin A C L, Maddocks O D K, Chokkathukalam A, Coyle J E, Jankevics A, Holding F P, Vousden K H, Frezza C, O'Reilly M, Gottlieb E. Serine is a natural ligand and allosteric activator of pyruvate kinase M2. *Nature*, 2012, 491(7424): 458–462
41. Yeh C M, Wang J P, Lo S C, Chan W C, Lin M Y. Chromosomal integration of a synthetic expression control sequence achieves poly- γ -glutamate production in a *Bacillus subtilis* strain. *Biotechnology Progress*, 2010, 26(4): 1001–1007
42. Sha Y Y, Sun T, Qiu Y B, Zhu Y F, Zhan Y J, Zhang Y T, Xu Z Q, Li S, Feng X H, Xu H. Investigation of glutamate dependence mechanism for poly- γ -glutamic acid production in *Bacillus subtilis* on the basis of transcriptome analysis. *Journal of Agricultural and Food Chemistry*, 2019, 67(22): 6263–6274
43. Fukushima T, Uchida N, Ide M, Kodama T, Sekiguchi J. DL-endopeptidases function as both cell wall hydrolases and poly- γ -glutamic acid hydrolases. *Microbiology (Reading, England)*, 2018, 164(3): 277–286
44. Hoffmann S L, Jungmann L, Schiefelbein S, Peyriga L, Cahoreau E, Portais J C, Becker J, Wittmann C. Lysine production from the sugar alcohol mannitol: design of the cell factory *Corynebacterium glutamicum* SEA-3 through integrated analysis and engineering of metabolic pathway fluxes. *Metabolic Engineering*, 2018, 47: 475–487
45. Israelsen W J, Vander Heiden M G. Pyruvate kinase: function, regulation and role in cancer. *Seminars in Cell & Developmental Biology*, 2015, 43: 43–51
46. Sonenshein A L. Control of key metabolic intersections in *Bacillus subtilis*. *Nature Reviews. Microbiology*, 2007, 5(12): 917–927
47. Yu W, Chen Z, Shen L, Wang Y, Li Q, Yan S, Zhong C J, He N. Proteomic profiling of *Bacillus licheniformis* reveals a stress response mechanism in the synthesis of extracellular polymeric flocculants. *Biotechnology and Bioengineering*, 2016, 113(4): 797–806